



# **Parametric Study of Spar Platform Responses**

By

Nony Motimbun

Supervised by

Mr. Mohamed Mubarak Bin Abdul Wahab

Dissertation submitted in partial fulfillment of  
the requirements for the  
Bachelor of Engineering (Hons)  
(Civil Engineering)

JUNE 2010

Universiti Teknologi PETRONAS,  
Bandar Seri Iskandar,  
31750 Tronoh ,  
Perak Darul Ridzuan.

# **CERTIFICATION OF APPROVAL**

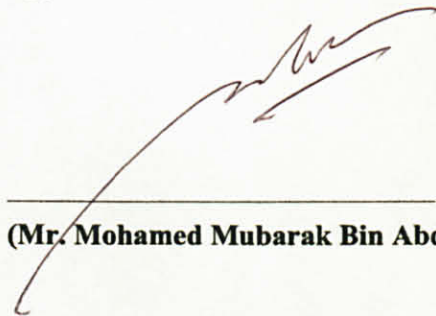
## **Parametric Study of Spar Platform Responses**

By

**Nony Motimbun**

A project dissertation submitted to the  
Civil Engineering Programme  
Universiti Teknologi PETRONAS  
in partial fulfillment of the requirement for the  
**BACHELOR OF ENGINEERING (Hons)**  
**(CIVIL ENGINEERING)**

Approved by,



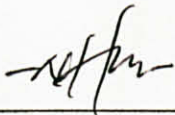
---

**(Mr. Mohamed Mubarak Bin Abdul Wahab)**

Universiti Teknologi PETRONAS,  
Bandar Seri Iskandar,  
31750 Tronoh,  
Perak Darul Ridzuan.

## CERTIFICATION OF ORIGINALITY

This is to certify that I am responsible for the work submitted in this project, that the original work is my own except as specified in the references and acknowledgements, and that the original work contained herein have not been undertaken or done by unspecified sources or persons.



---

**(NONY MOTIMBUN)**

10<sup>th</sup> JUNE 2010.



## ABSTRACT

Since the first spar platform was installed in Gulf of Mexico (GOM) in 1996, spar platform has been regarded as competitive floating structure for deep-sea oil exploration. In this study, dynamic analysis is applied to measure the responses of a typical spar platform in order to measure instantaneous amplitude and frequency fluctuations of three degrees freedom (surge, heave and pitch). The analysis was performed for a spar subjected to random wave loading represent an operational condition of 100-year storm in Gulf of Mexico. The first part of this project focuses on the detailed information of the chosen existing spar. Next, the evaluation of the responses using mathematical calculations and it is modeled as a rigid body connected to the sea floor by multi component catenaries mooring lines. Frequency domain analysis has been performed by choosing P-M Spectrum model to represent an appropriate density distribution of seawater at the site under consideration. The parameters chosen for assessing the responses are the stiffness that varies  $\pm 10\%$  of original stiffness and different condition of hydrodynamic coefficients (Clean and Fouled). From the analysis, the response increases when the stiffness was lower and decreased when the stiffness is higher than the original. The smaller value of hydrodynamic coefficient affects the spar motion by decreasing it. The results presented in this paper will provide an insight to the differences in Spar motion responses due to the variation in both design parameters. The findings should be beneficial for spar design in an early project stage.

## **ACKNOWLEDGEMENTS**

I would like to take this opportunity to thank various people who have helped me throughout the period of completing my Final Year Project I and II. First of all, my utmost appreciation and heartfelt thanks to Mr. Mohamed Mubarak Bin Abdul Wahab, my FYP supervisor, also, thank you for the support and the time he managed to spend in answering my question and feed my curiosity. Secondly, my deepest gratitude to Professor Dr. Kurian. V. John for helpful guidance, advices and encouragement that have truly been a great inspiration to me. I also would like to deliver my special gratitude to my fellow colleagues for sharing their invaluable knowledge and expertise to help in this project.

Last but not least, to everyone who have assisted me directly or indirectly in making sure my Final Year Project a successful one.

## TABLE OF CONTENTS

<b><u>CHAPTER</u></b>	<b><u>PAGE</u></b>
<b>CERTIFICATION OF APPROVAL .....</b>	<b>i</b>
<b>CERTIFICATION OF ORIGINALITY .....</b>	<b>ii</b>
<b>ABSTRACT .....</b>	<b>iii</b>
<b>ACKNOWLEDGEMENTS .....</b>	<b>iv</b>
<b>LIST OF TABLES .....</b>	<b>v</b>
<b>LIST OF FIGURES .....</b>	<b>vi</b>
<b>CHAPTERS</b>	
<b>CHAPTER 1 – INTRODUCTION .....</b>	<b>1</b>
1.1 – Background .....	1
1.2 – Problem Statement .....	2
1.3 – Objective .....	3
1.4 – Scope of study .....	3
<b>CHAPTER 2 – LITERATURE REVIEW/THEORY .....</b>	<b>4</b>
2.1 – Spar .....	4
2.2 – Truss Spar .....	4
2.3 – Frequency Domain Analysis Vs Time Domain Analysis .....	4
2.4 – Hydrodynamic coefficient .....	5
2.5 – Analysis of spar buoy .....	5
2.6 – Spar Responses .....	6
2.7 – Pierson-Moskowitz Spectrum .....	7

2.8 – Wave Force and Moment Calculation .....	7
2.9 – Frequency Domain Analysis.....	10
2.10 – Wave Spectrum.....	11
2.11– Motion Response Spectrum .....	12
2.12– Added Mass and Damping Coefficient.....	13
<b>CHAPTER 3 – METHODOLOGY .....</b>	<b>14</b>
3.1 – Flow Chart .....	14
3.2 – Structural Model .....	15
3.3 – Theoretical Dynamic Analysis.....	20
3.3.1 – Wave Force and Moment Calculation .....	20
3.3.2 – Wave Spectrum.....	21
3.3.3 – Motion Response Spectrum .....	21
3.3.4 – Parametric Analysis .....	22
<b>CHAPTER 4 – NUMERICAL RESULT AND DISCUSSIONS .....</b>	<b>23</b>
4.1 – Wave Spectrum.....	23
4.2 – Response of Truss Spar (Hard Tank) on	
Surge, Heave and Pitch .....	24
4.2.1 – Surge .....	25
4.2.2 – Heave .....	27
4.2.3 – Pitch .....	28
4.3 – Discussion .....	30



<b>CHAPTER 5 – CONCLUSION.....</b>	<b>31</b>
<b>CHAPTER 6 – ECONOMICAL BENEFITS.....</b>	<b>32</b>
<b>CHAPTER 7– REFERENCES .....</b>	<b>34</b>
<b>APPENDICES .....</b>	<b>35</b>
Appendix I – Wave Data.....	36
Appendix II – Wave Spectrum .....	39
Appendix III – Wave Calculation	
Total Horizontal Force For Hard Tank .....	41
Appendix IV – Heave Analysis .....	44
Appendix V – Pitch Analysis	
i) Moment Calculation	
ii) RAO Moment Calculation.....	48



## LIST OF TABLE

	<b><u>PAGE</u></b>
1. Table 1: Dimension and wave data	18
2. Table 2: Responses in variation of Stiffness	24
3. Table 3: Responses in variation of hydrodynamic coefficient	24
4. Table 4: Construction cost comparison	33

## LIST OF FIGURES

	<b><u>PAGE</u></b>
1. Figure 1 : Classic Spar	2
2. Figure 2 : Truss Spar	2
3. Figure 3: Definition Sketch for wave forces	8
4. Figure 4: Wave Spectrum	11
5. Figure 5: Computer model of Holstein Spar	16
6. Figure 6: Spar Degree of freedom	17
7. Figure 7: Axis coordinate system	19
8. Figure 8: PM Spectrum	23
9. Figure 9: Simulated wave profile	23
10. Figure 10: Surge Response Spectrum (1)	25
11. Figure 11: Simulated Surge Profile (1)	25
12. Figure 12: Surge Response Spectrum (2)	26
13. Figure 13: Simulated surge profile (2)	26
14. Figure 14: Heave response spectrum	27
15. Figure 15: Simulated heave profile	27

16. Figure 16: Pitch response spectrum (1)	28
17. Figure 17: Simulated pitch profile (1)	28
18. Figure 18: Pitch response spectrum (2)	29
19. Figure 19: Simulated pitch profile (2)	29
20. Figure 20: Comparison of construction time between spar	30

and Dry tree semisub

## **CHAPTER 1**

### **1. INTRODUCTION**

#### **1.1 Background**

Spar platform is one of offshore floating structure used for deepwater applications for the drilling, production, processing, storage and offloading of ocean deposits. When water depth exceeds from a specific level, spar becoming one of the economic choices because of its simple shape and structure. Its four major systems are hull, moorings, topsides and risers. The top part of the hull provides buoyancy and the middle section provides plenty room for oil storage. The lower compartment holds the ballast, which control the trim for spar. There are two types of spar, classic and truss spar. Classic spar is a deep draught, vertical, large diameter cylindrical vessel. The truss spar is used when the midsection is not needed for oil storage. The midsection is replaced with a truss framework and plated horizontal levels. The effective vertical mass of structure is up to the same level as the classic spar. Advantages of using spar compared to the other floating structures includes structural simplicity, low motions in moderate and extreme ocean waves, good protection of risers connections to the seabed and more economical.



*Figure 1 : Classic Spar*



*Figure 2 : Truss Spar*

## **1.2 Problem Statement**

World population increases with rapid economics developments in recent decade and more requests for oil results in the increase of oil price. With the advanced technology, oil production in the sea depths becomes more and more economics. Developing countries emphasizing on the deeper zones for discovering new sources. Platforms, FPSO, TLP and spar are examples of platform used for deeper zones.

Further study in spar platform will be beneficial to both Universiti Teknologi Petronas and PETRONAS as the research provides theoretical knowledge at this subject. A lot of money is involved for maintaining and fixing offshore platform, by the end of this research; the information can be used for consultancy purposes.



### 1.3 Objectives

The objectives of this study are:

- a. Select and finalize the dimension of typical spar platform for this project.
- b. Complete a dynamic analysis of this typical spar platform due to random waves in the variation of the stiffness, K value with  $\pm 10\%$  of its original stiffness and hydrodynamic coefficient and determine the motion responses .

### 1.4 Scope of Study

The analyses used in this study are:

- a. Frequency domain analysis

Frequency domain is used to solve dynamic responses. The analysis is performed for the linearised problem.

- b. Morison Equations

Evaluation of the horizontal wave forces acting of the spar, which assume extends from the bottom through the free surface. Calculated force will be used to analyze the Response Amplitude Operator.

- c. Wave Spectra

Determine responses of the spar towards the motion of surge, heave and pitch by multiplication of the wave energy spectrum with  $RAO^2$  to evaluate the response spectrum value at particular frequency.

## CHAPTER 2

### 2. LITERATURE REVIEW/THEORY

#### 2.1. Spar

A spar is deep-draft floating caisson, which is a hollow cylindrical structure similar to a very large buoy. The spar relies on a traditional mooring system to maintain its position. About 90 percent of the structure is underwater.[[www.globalsecurity.com](http://www.globalsecurity.com)] The distinguishing feature of a spar is its deep-draft hull, which produces very favourable motion characteristics compared to other floating concepts. Low motions and a protected centerwell also provide an excellent configuration for deepwater operations. Water depth capability has been stated by industry as ranging up to 3048m.[[Wikipedia.com](http://Wikipedia.com)]

#### 2.2. Truss spar

Several studies revealed that the truss spar is better than classic spar in that it offers lower cost, lower weight, shorter construction duration, dampened heave motion, less drag provided by the truss and reduced overall mooring system loads in high current environment. The upper part of the truss spar consists of a relatively shallower hard tank and is connected to a truss structure with a number of heave plates. The multiple heave plates greatly increased the heave added mass and viscous damping, which contributes to minimize the heave motion despite the increase of the heave wave exciting force due to shallower cylinder draft. Some experiments have been conducted and the results showed the truss spar exhibited excellent motion characteristics [[Halkyard,2002](#)].

#### 2.3. Frequency Domain Analysis Vs Time Domain Analysis

According to **V.J Kurian**, results of numerous hydrodynamics analysis and motion response predictions technique have been developed and introduced in various paper. Generally, there are two basic approaches used in performing dynamic

analysis of floating structures; frequency domain and time domain analysis. The frequency domain analysis is less time consuming and simpler compared to time domain analysis because the response estimation can be carried out using wave spectrum method. However, there is a limitation for the frequency domain analysis that all nonlinearities in the equation of motion are replaced by the linear approximations where it will lead to low accuracy and error in response prediction. The nonlinearities are in fluid drag force, mooring line force, viscous damping and stiffness of the system for different motions consideration. Another study by **Weggel et al** uses the frequency domain technique and directly gives the statistical parameters of the spar response at relatively low comparison cost. However it may be subject to large errors due to the linearization of some non-linear terms, such as the viscous term, in the equations of motion. There is evidence that this linearization probably overestimates viscous effects.

#### **2.4. Hydrodynamic Coefficient**

Research by **Sarpkaya, 1976** showing that hydrodynamic coefficient  $C_m$  and  $C_D$  for cylinder are functions of  $Re$ . Typical results for  $C_m$  and  $C_D$  obtained approaches 1.8 and 0.65 respectively. Wave tank test by **Chakrabati, 1980** on a vertical cylinder have produced results on  $C_m$  and  $C_D$  that are comparable to Sarpkaya's at corresponding  $Re$  number. The forces due to regular waves on a small section of the cylinder were measured from which the values of the hydrodynamic coefficient were derived by the least square method.

#### **2.5. Analysis of Spar buoy**

Simulation of the motion of a spar buoy requires the definition of the equations of motion and the evaluation of all forces acting on it due to wind, current ocean waves and mooring lines. The conventional approach in offshore engineering is to use the linear form of the equations to describe the motions of rigid bodies. For large motions, the non-linear equations of motion [**Chitrapu et al**] should be used. A key element of the analysis of a spar buoy is to evaluate the forces and moments on it due to ocean waves and currents. One possibility to obtain these is to perform a



numerical analysis of the fully non-linear interaction between spar and its surrounding fluid. Although it is not impossible, this task requires very powerful computer resources and is therefore not feasible in practice.

## 2.6. Spar responses

Lyle Finn, Tim Weaver, 2000 believe that the primary cause of the reduced heave was damping forces such as friction between the risers and the supporting guides and mooring line dynamic drag that were unaccounted for. A new analysis capability was subsequently developed to simultaneously predict the dynamic response of the vessel, mooring lines and risers. Results of the coupled analysis reveal that mooring line dynamics and riser friction have significant effect on the spar heave response. As a result of reduction in heave response, the draft of the spar can be reduced.

A characteristic featured of moored offshore structures such as a Spar platform is their slow oscillatory motion that occurs at resonance frequencies, well beyond the frequency range of the wave spectrum. Since the damping of such structures is low at resonant periods, correct estimation of damping is important in predicting the motions, maximum offsets and extreme mooring loads. Generally, response of spar platforms is predicted conservatively by excluding the damping from mooring lines and risers.

Damping from risers on the spar platform occurs from coulomb friction at the riser guides and keel as well as from the hydrodynamic viscous effects. The risers exert a normal force at the keel guide and other air can guide locations. As the spar pitches laterally, the riser induced normal reaction increases. As the spar heaves vertically, a friction force is developed on the guides, which is proportional to normal reaction from the risers and depends on the coefficient of friction. If the spar vertical motion is small enough, the static friction will prevent the spar from moving further.

When the spar motions are larger, the kinetic friction opposes the motion and thus produces damping. In addition to the damping, coupling forces between the riser and the Spar arise in both surge/sway motions as well as pitch/roll motions. The buoyancy force of the riser air cans provide additional restoring moments that affect

the pitch/roll motions. The riser lateral reaction at the keel and other guide locations affects the surge/sway motions. Current drag on risers, if significant, produces additional lateral reaction at the keel which can affect both surge/sway and pitch/roll motions.

According to **Wang Ying, Yang Jian-min**, in extreme condition at Gulf of Mexico, the maximum value of surge is less than 1% of the water depth, the heave motion is effectively controlled in the range of 10% of the significant wave height, and the natural frequencies of pitch are far away from the peak frequency of wave spectrum.

## **2.7. Pierson-Moskowitz spectrum**

The P-M spectral model describes a fully-developed sea determined by one parameter, namely, the wind speed. The fetch and duration are considered infinite. For the applicability of such model, the wind has to blow over a large area at a nearly constant speed for many hours prior to the time when the wave record is obtained and the wind should not change its direction more than a certain specified small amount. In spite of these assumptions, the P-M model has been found to be useful in representing a severe storm wave in offshore structure design [S.K Chakrabati,2001]

## **2.8. Wave Force and Moment Calculation**

The Morison's Equation was developed by Morison, O'Brien, Johnson and Shaaf in describing the horizontal wave forces acting on a vertical pile which extend from the bottom through the free surface. Morison proposed that the force exerted by unbroken surface waves on a vertical cylindrical pile which extends from the bottom through the free surface is composed of two components, inertia and drag.



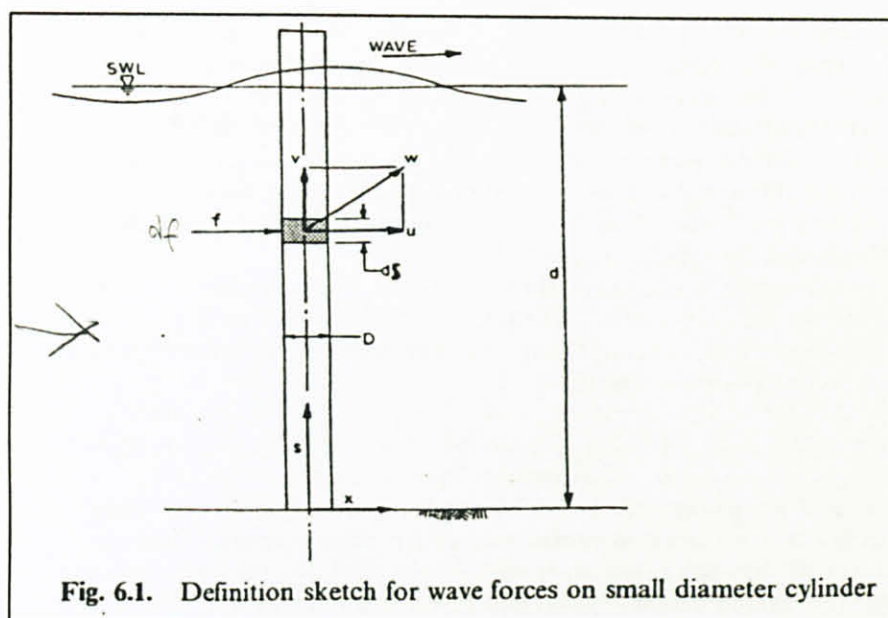


*Figure 3: Definition Sketch for wave forces*

The computation of the water wave forces on an offshore structure is one of the primary tasks in the design of structure. The wave forces are developed because of the motion of water particles hitting the structure with velocities and accelerations. In this case, the calculation for Truss part are not necessary as it contributes insignificant forces.

The principle involved in the concept of the inertia force is that a water particle moving in a wave carries a momentum with it. As the water particle passes around the circular cylinder it accelerates and decelerates. This requires that work be done through the application of a force on the cylinder to increase this momentum. The incremental force on a small segment of the cylinder,  $dl$ , needed to accomplish this is proportional to the water particle acceleration at the center of the cylinder (in the absence of the cylinder).

Morison's equation expresses the wave force as the sum of an inertia force proportional to the particle acceleration and a non linear drag force proportional to the square of the particle velocity:

$$F = F_I + F_D \quad (1)$$

$$F = C_M \frac{\rho \pi D^2}{4} u' + C_D \frac{\rho D}{2} |u| u \quad (2)$$

$F$  = wave force per unit length on a circular cylinder

$u$  = water particle velocity normal to the cylinder

$u'$  = water particle acceleration normal to the cylinder

$\rho$  = sea water density

$D$  = member diameter

$C_D$  AND  $C_M$  = drag and inertia coefficients, respectively.

By using linear wave theory, with a wave height and wave period chosen according to the location of the structure, the corresponding horizontal and vertical components of wave particle velocity and acceleration were determined. The kinematics of the wave water were determined by the following equations:

$$\text{Horizontal Water Particle Velocity :} \quad u = \frac{\pi H}{T} \frac{\cosh ks}{\sinh kd} \cos \theta \quad (3)$$

$$\text{Vertical Water Particle Velocity :} \quad v = \frac{\pi H}{T} \frac{\sinh ks}{\sinh kd} \sin \theta \quad (4)$$

$$\text{Horizontal Water particle Acceleration :} \quad u' = \frac{2\pi^2}{T^2} H \frac{\cosh ks}{\sinh kd} \sin \theta \quad (5)$$

$$\text{Horizontal Water particle Acceleration :} \quad v' = -\frac{2\pi^2}{T^2} H \frac{\sinh ks}{\sinh kd} \cos \theta \quad (6)$$

$$s = y + d$$

$$\theta = kx - \omega t$$

$$k = \frac{2\pi}{L}$$

$$\omega = \frac{2\pi}{T}$$

T = wave height

y = height of the point of evaluation of water particle kinematics

x = point of evaluation of water particle kinematics from the origin on the horizontal direction

t = time instant at which water particle kinematics is evaluated

L = wave length

H = wave height

d = water depth

## 2.9. Frequency Domain Analysis

Frequency domain analysis was performed first by choosing a suitable wave spectrum model to represent an appropriate density distribution of sea wave at the site under consideration. The analysis was performed in the frequency domain. Secondly, the motion-response spectrum was determined based on the wave spectrum for the response in surge, heave and pitch degrees of freedom. Finally, the motion response profile was simulated from the motion spectrum.

## 2.10. Wave Spectrum

The expression for P-M spectrum in terms of cyclic frequency  $f \left( \frac{\omega}{2\pi} \right)$  may be written as

$$S(f) = \frac{\alpha g^2}{2\pi^4} f^{-5} \exp \left[ -1.25 \left( \frac{f}{f_0} \right)^{-4} \right] \quad (7)$$

$$\alpha = 0.0081, \text{ Peak frequency} = f_0 \left( \frac{\omega_0}{2\pi} \right)$$

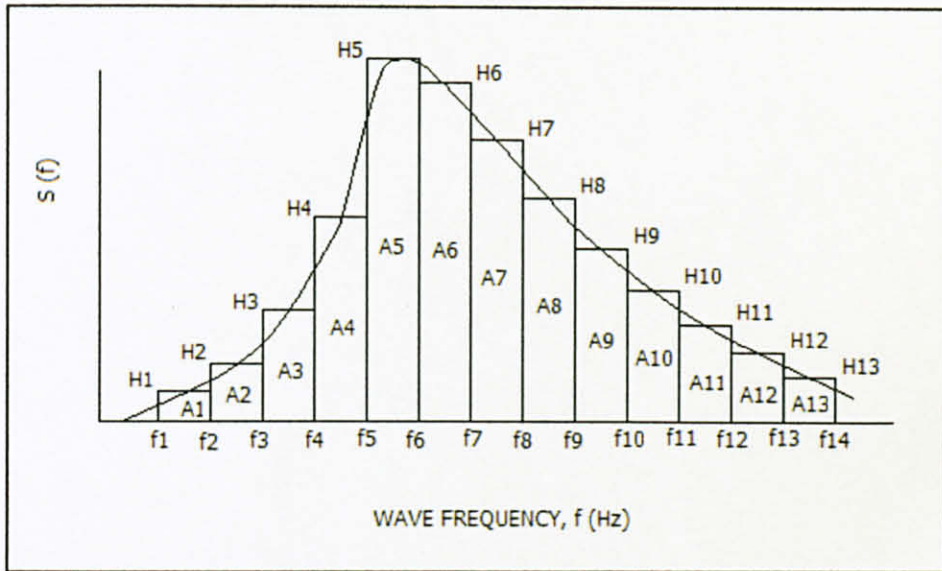


Figure 4: Wave Spectrum

Relationship between the peak frequency and the significant height for the wave was as follows;

$$\omega_0 = 0.161g/H_s \quad (8)$$

The weight height at  $f_1$ ,

$$H(f_1) = 2\sqrt{2(f_1)\Delta f} \quad (9)$$

Time history of the wave profile was determined from:

$$\eta(x,t) = \sum_{n=1}^N \frac{H(n)}{2} \cos[k(n)x - 2\pi f(n)t + \varepsilon(n)]$$

### 2.11. Motion Response Spectrum

The responses of the spar towards the motion of surge, heave and pitch are calculated by multiplication of the wave energy spectrum (7) with  $RAO^2$  to evaluate the response spectrum value at particular frequency. The expression of motion-response spectrum may be written in the following form (12) and (13) :

$$RAO = \frac{\frac{F_I}{H/2}}{\sqrt{[(K - m\omega^2)^2 + (C\omega)^2]}} \quad (11)$$

$$S_x(f) = [RAO(\omega)]^2 S(f) \quad (12)$$

$$S_x(f) = \left[ \frac{\frac{F_I}{H/2}}{\sqrt{[(K - m\omega^2)^2 + (C\omega)^2]}} \right]^2 S(f) \quad (13)$$

RAO is defined as response amplitude per unit wave height.

$F_I$  = Inertia force

$K$  = Stiffness

$M$  = summation of mass and added mass

$C$  = structural damping

$H$  = wave height

$\omega$  = natural frequency corresponding to particular frequency.



## 2.12. Added mass and Damping Coefficient

The added mass concept arises from the tendency of a submerged body moving acceleration relative to the surrounding fluid to include acceleration to the fluid. These fluid accelerations require forces which are exerted by the body through a pressure distribution of the fluid on the body. For computed added mass coefficients, the truss spar divided into three sub structures: hull, truss and heave plates.

The added mass force of circular cylinder with length  $l$  when given normal acceleration  $a_N$  is

$$F_N^A = A_F \cdot l \cdot a_N$$

Where,

$$A_F = C_a \cdot \rho \cdot \pi \cdot r^2$$

$A_F$  = added mass per unit length of a circular cylinder

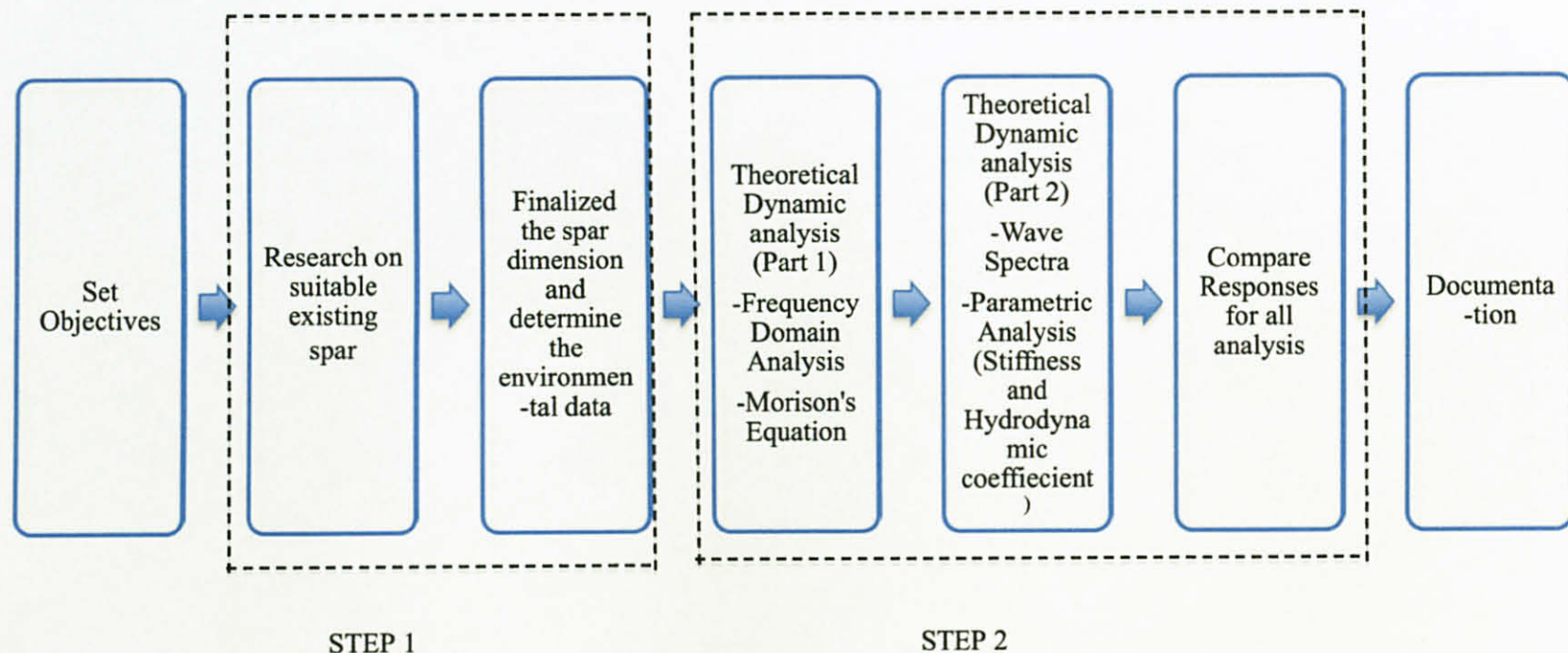
$r$  = radius

$C_a$  = added mass coefficient

$\rho$  = density of water

3. METHODOLOGY

Flow Chart



### **3.2. Structural Model**

By considering the availability of resources and most studied spar, the typical spar chosen is Holstein Spar. Holstein truss spar, the largest ever built, was designed and constructed in 35 months. Due to its size, the hull could not be transported in single piece; it was constructed in two yards. The truss spar lays approximately 240km South of New Orleans in Green Canyon block 645. It was discovered in 1999 adjacent to the Mad Dog and Atlantis fields. Holstein is being developed using a Production Drilling and Quarters (PDQ) truss spar, permanently moored. Gulf of Mexico is predominated by loop and eddy currents generated by Gulf Stream. These currents resulted in; the largest mooring system ever installed for a spar, the heaviest and longest suction piles as well as considerable challenges over hull (hard tank) responses.

The resulting Holstein hull displacement is 105,000 tons, the largest for any spar ever built. In comparison, the first production spar, Neptune, could fit inside the center well of Holstein. The hull consists of a truss spar with a 16 leg mooring system. The diameter of the hard tank section is 46m and the length is 89m. The truss is 131m long with a soft tank 7.62m. The mooring systems which control the stiffness and buoyancy of the spar consists of 16 suction piles 5.5m and 39m long. They are attached to the spar hull via a ground chain attached to two segments of spiral strand wire and an upper platform.

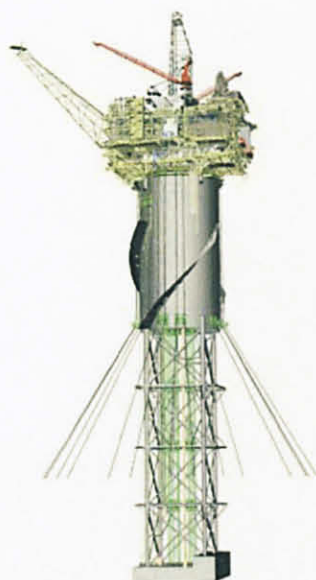


*Figure 5: Computer model of Holstein Spar*

To accommodate extra payload from the risers without significantly increasing the hull size, it was decided to install all 15 risers before the first hurricane season. This resulted in a significant reduction of the fixed ballast, leading the reduced hull motion and enhanced hull weight optimization. This is achieved by taking advantage of the riser's restoring forces, weight and pretension, all effectively acting at the keel. The increased vertical stiffness of the platform, reduced the heave natural period closer to wave period.

The truss spar consists of topside located above the hard tank. In this study, only calculation for hard tank is considered as several studies has performed to conclude that there is no significant forces at the truss part of the spar. The Holstein hard tank is the first to utilizes access shafts to access all internal void and ballast tanks hence eliminating the need to go through all upper tanks to reach one of the lower tanks, reducing the risk of multiple tanks flooding due to several open tanks, allowing or facilitating the installation and commissioning of all piping in one area of the hull, reducing the amount of scaffolding required during fabrication. With the Holstein hard tank not having any buoyancy can guide structure when compared to previous spar, center well sloshing became a major concern in calculating load and risers and center well piping.



The truss spar was modeled as a rigid body with three degree of freedom (surge, heave, pitch) at its centre of gravity, connected to the seafloor by 16 mooring lines. The mooring line held the platform in place. The centre of gravity of spar is above the centre of buoyancy to provide inherently stable design for spar.

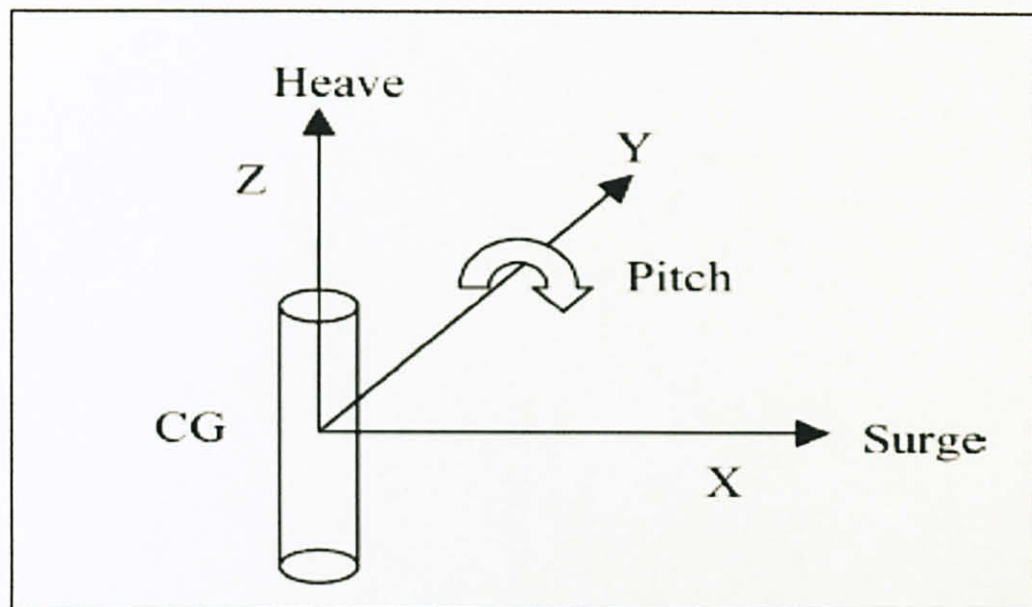


*Figure 6: Spar Degree of freedom*

The principle dimensions of the typical spar hull and wave data are given in the table below.

*Table1: Dimension and wave data*

Hull Length, m	227
Diameter, m	46
Total draft, m	73
Wave period, s	16.7
Wave height, m	23.2
Water depth, m	1325
Drag coefficient ( $C_D$ ) GOM extreme	0.7
Inertia coefficient ( $C_M$ )GOM extreme	2.0
Drag coefficient ( $C_D$ ) Clean	0.65
Inertia coefficient ( $C_M$ )Clean	1.60
Drag coefficient ( $C_D$ ) Fouled	1.05
Inertia coefficient ( $C_M$ )Fouled	1.20
Structural Damping Ratio	0.05

The platform global analysis axis system used for the calculation of wave forces and moment. All locations are specified based on this coordinate system. The origin was taken at the Longitudinal/Transverse Centerline at the top of Hard Tank with the Y-axis positive up. The longitudinal axis (X-axis) was along platform East-West with positive towards East. The transverse (Z-axis) direction was along platform North-South with positive North.

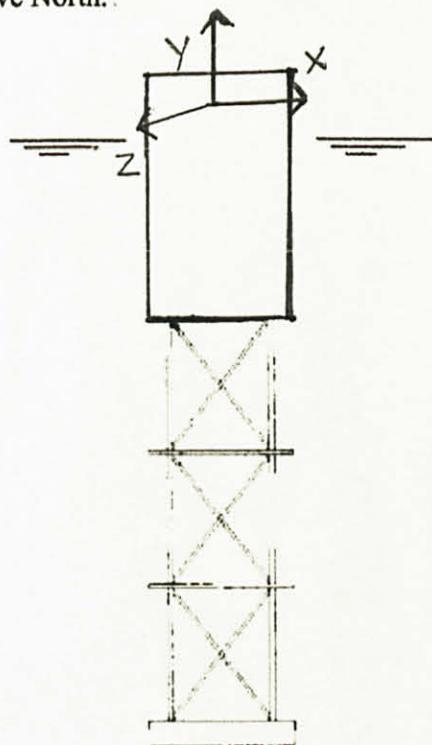


*Figure 7: Axis coordinate system*

### 3.3. Theoretical Dynamic Analysis

#### 3.3.1. Wave Force and Moment Calculation

The wave force acting on the spar is the important of all environmental loading. The calculation of wave loads on the truss spar is based on Morison's equation applied in conjunction with linear wave theory. Truss spar is considered as hydro-dynamically transparent with no significant influence on the wave field. It is because the ratio of the truss spar diameter to wave length is small ( $D/L < 0.2$ , where  $D$  is the structure diameter and  $L$  is the wave length)

- i) The reference point ( $x=0$ ) is considered for the wave such that at  $x=0$ , the surface profile becomes equal to  $H/2$  when the time,  $t=0$ . First order velocity potential,  $\Phi$  becomes

$$\Phi = \frac{\pi H \cosh ks \sin \Theta}{kT \sinh kd} \quad (14)$$

While the wave length is obtained from the formula

$$L = \frac{gT^2 \tanh kd}{2\pi} \quad (15)$$

- ii) By differentiating Equation 14 with respect to  $x$  and  $y$  respectively, the horizontal and vertical velocity (Equation 3 and 4) are obtained.

The truss spar was divided into 2 sections including hard tank and truss section. The wave was assumed in  $X$  direction and the entire truss spar structure was considered vertical in place, no inclination in  $Y$  axis. Heave plates and soft tank were not included in the wave forces calculation because their sizes and orientation contributed only insignificant wave forces. The wave forces calculated using Morison's Equation (Equation 1 and 2) with  $C_m=2.0$  and  $C_d=0.7$  at the hard tank of the spar. The wave force was assumed to act at the origin,  $x$  ( $x = 0m$ ) and when the time,  $t$  is equal to  $0s$ .



### 3.3.2. Wave spectrum

The spectrum chosen is P-M Spectrum. The wave energy density spectrum,  $S(f)$  was determined based on the Equation (7) and the significant height was obtained from wave record of  $H_s=12.4\text{m}$ . The P-M spectrum was drawn range from the frequencies of 0.005 Hz to 0.295 Hz with a frequency increment,  $\Delta f$  of 0.01 Hz and the corresponding wave height was obtained using Equation (9). From the calculated wave height and Equation (10), the time history of the wave profile ( $t=0$  seconds to  $t=100$ seconds) in front of truss spar at  $x=0\text{m}$  was computed and a random phase in the range of  $(0, 2\pi)$  was assigned to a random number generator,  $R_N$  to retain randomness of the time history.

With  $H_s=12.4\text{m}$ ,  $\Delta f = 0.01$  Hz, the natural frequency was obtained from Equation 8. The weight height at frequency  $f_1$  was derived from Equation 9 and the time history were constructed with referring to the Equation 10, where  $x$  was the location of evaluation of wave profile from the origin in the horizontal direction;  $t$  was the time instant at which wave profile was evaluated and was incremented; wave number  $k(n)$ ; wave length  $L(n)$  corresponded to the wave length for  $n$ th frequency  $f(n)$ ; wave height  $H(n)$  was computed from Equation 9 for  $n$ th frequency; and the total number of frequency band of width  $\Delta f$ , dividing the total energy density.

### 3.3.3. Motion Response Spectrum

The responses of the spar towards the motion of surge, heave and pitch are calculated by multiplication of the wave energy spectrum (7) with  $\text{RAO}^2$  to evaluate the response spectrum value at particular frequency. The motion response spectrum were written in form of Equation 11,12 and 13, where RAO was amplitude of response per unit wave amplitude;  $F_1$  was inertia force;  $K$  was stiffness of the structure associated with different type of motion;  $m$  was summation of mass and added mass of the structure associated with different type of motion;  $C$  was structural damping ratio which is equal to 5%;  $H$  was wave height corresponding to particular frequency; and  $\omega$  was natural frequency corresponding to particular frequency.

From the resulting motion-response spectrum, the expected response (time history) profiles in 200 seconds were created. Equation 10 was used to construct the response time series.

#### **3.3.4. Parametric Analysis**

For this study, two important parameters in spar platform were chosen; stiffness and hydrodynamic coefficient. The stiffness was varied to  $\pm 10\%$  of the original stiffness and there were three conditions considered in the hydrodynamic coefficient, namely GOM extreme, Clean and Fouled.

The analyses for stiffness parameter were conducted by changing the value of the total buoyancy of the structure by adding and deducting the K value in the following equation

$$\omega_n = \sqrt{\frac{K}{m}} \quad (16)$$

where K is the stiffness and m is the total mass.

The resulted value was then used in determining the correspondence responses.

In the analysis of hydrodynamic coefficient, the value of  $C_m$  and  $C_d$  in Morison's Equation were varied. GOM extreme was obtained from Chakrabati Offshore Handbook and both Clean and Fouled were found in API offshore handbook.

Motion spectrum from all the parameters were analyzed and compared to obtain the optimum response and the percentage difference.

# CHAPTER 4

## 4. NUMERICAL RESULTS AND DISCUSSIONS

### 4.1. Wave Spectrum

Based on Equation (7) and Equation (10), the stimulated wave profile is shown below. The maximum wave height was approximately 3.7m.

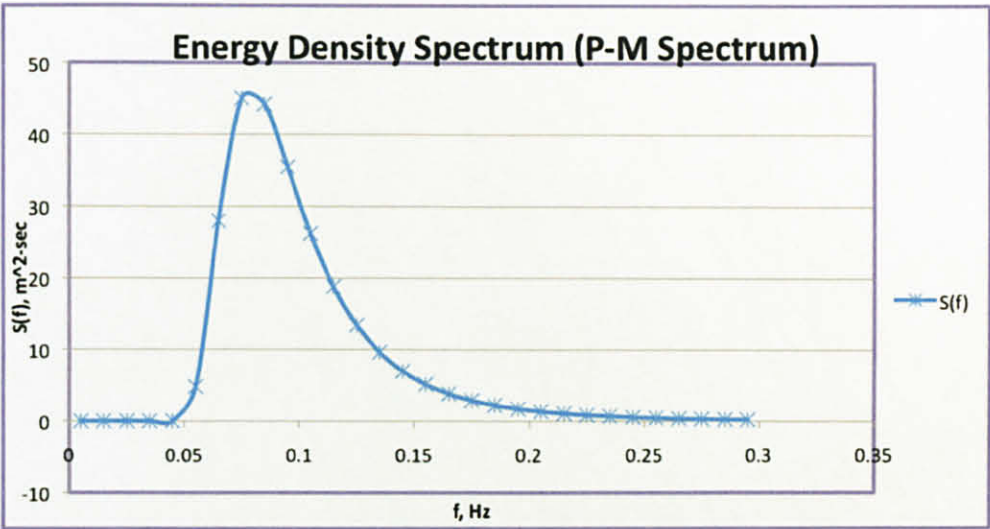


Figure 8: PM Spectrum

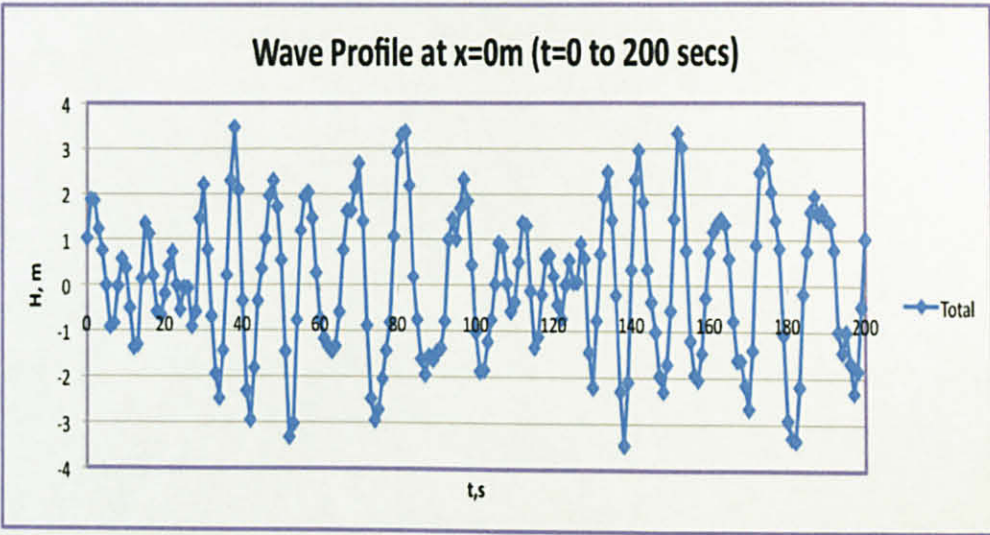


Figure 9: Simulated wave profile



#### 4.2. Response of Truss Spar (Hard Tank) on Surge, Heave and Pitch Motions

The responses of the structure are calculated with the variation in stiffness,  $K$  and hydrodynamic coefficient,  $C_m$  and  $C_d$ . The maximum amplitudes of the three motion responses were listed in the table:

*Table 2: Responses in variation of Stiffness*

STIFFNESS	SURGE (m)	HEAVE (m)	PITCH (rad)
K	0.207	0.0444	0.0259
+10%	0.187	0.0404	0.0238
-10%	0.228	0.0494	0.0264

*Table 3: Responses in variation of hydrodynamic coefficient*

HYDRODYNAMIC COEFFICIENT	SURGE (m)	HEAVE (m)	PITCH (rad)
$C_m=2.0$ , $C_d=0.7$ (Extreme Condition)	0.207	No significant forces	0.0259
$C_m=1.60$ , $C_d=0.65$ (Clean)	0.164	No significant forces	0.0214
$C_m=1.20$ , $C_d=1.05$ (Fouled)	0.124	No significant forces	0.0156



#### 4.2.1. Surge

Calculated surge response:

Variation of Stiffness

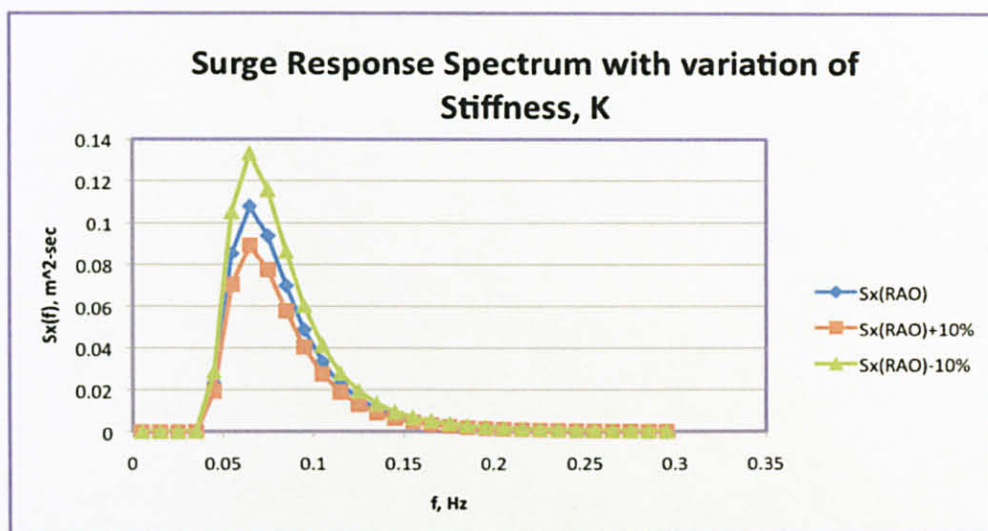


Figure 10: Surge Response Spectrum (1)

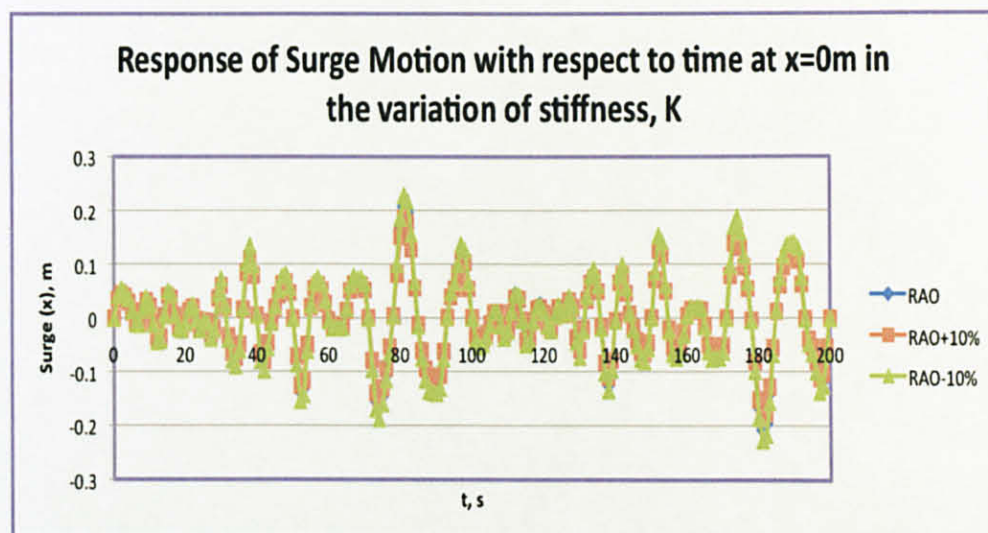


Figure 11: Simulated Surge Profile (1)

## Variation of Hydrodynamic coefficient

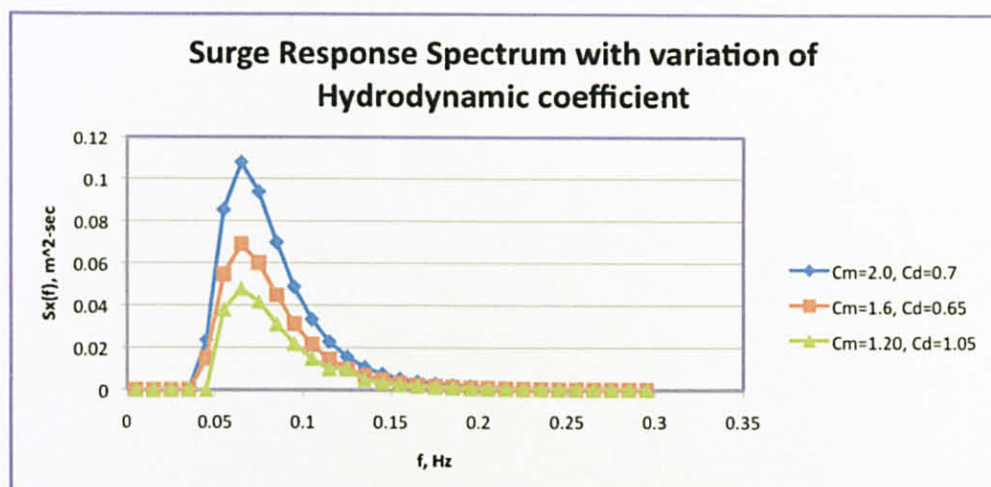


Figure 12: Surge Response Spectrum (2)

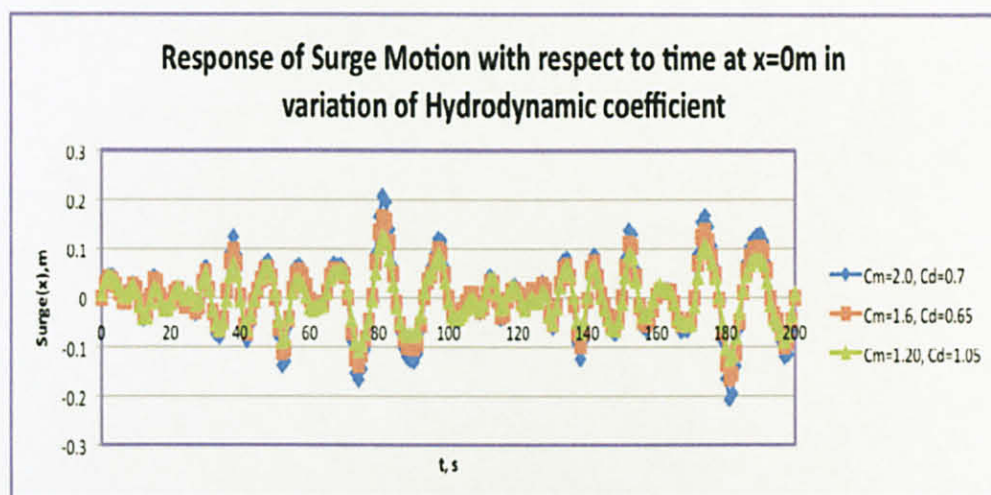


Figure 13: Simulated Surge Profile (2)

Based on the simulated wave profile, when the stiffness is varied, the amplitude changes. From Figure 11, the maximum amplitude is 0.228m at stiffness -10% of the original stiffness.. The response at +10%K decreased by 9.66% and value at +10%K increased 10.1%.

By observation on Figure 13, the maximum amplitude is 0.207m when the hydrodynamic coefficients equal to  $C_m=2.0$ ,  $C_d=0.7$ . The value of calculated

amplitude decreased by approximately 20.8% in Clean condition and 40% in Fouled condition.

4.2.2. Heave

Calculated heave response:

Variation of Stiffness

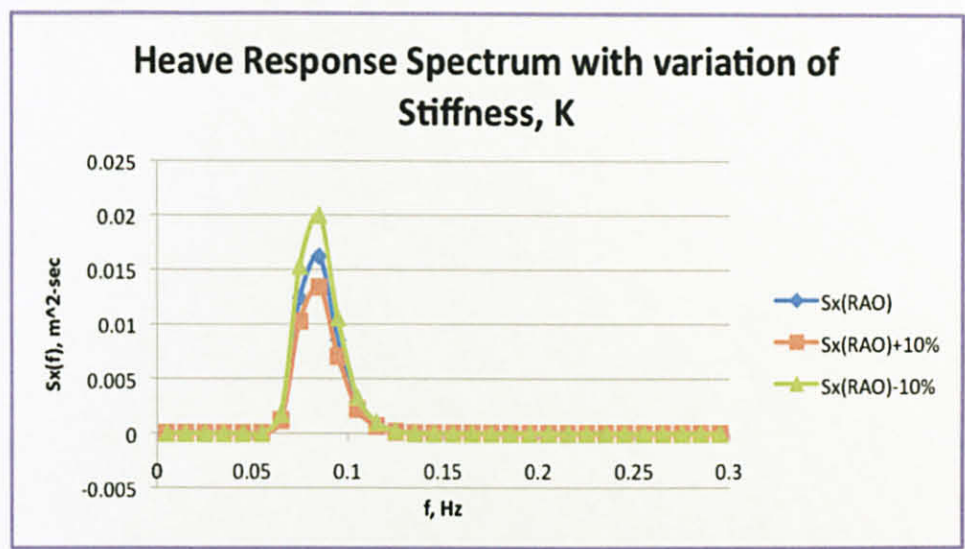


Figure 14: Heave Response Spectrum

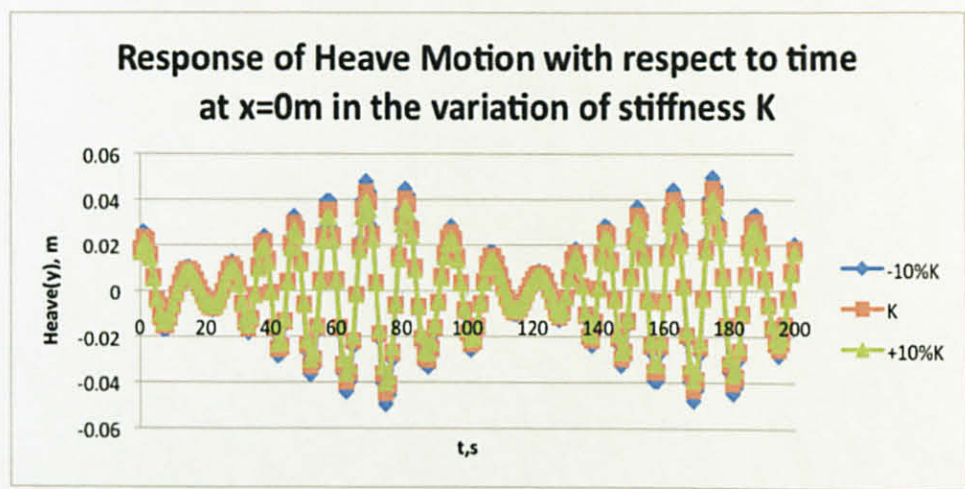


Figure 15: Simulated Heave Profile

In heave-simulated profile, the calculated maximum value is 0.0494m when the stiffness is less 10%, which is 11.3% larger than the original response. At stiffness +10% of the original stiffness, the response decreased by 9%. The hydrodynamic coefficient value contributes insignificant changes to the total response.

### 4.2.3. Pitch

Calculated pitch response:

Variation of stiffness

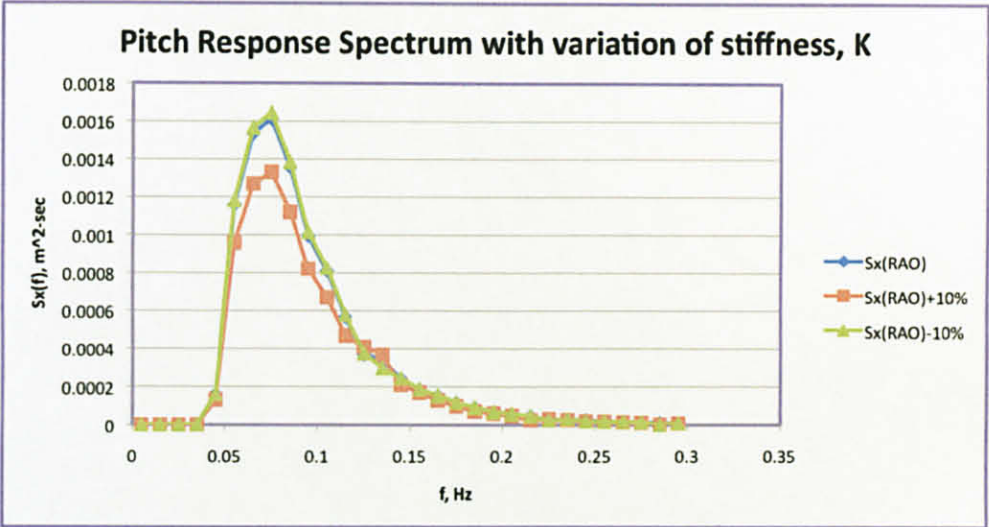


Figure 16: Pitch Response Spectrum (1)

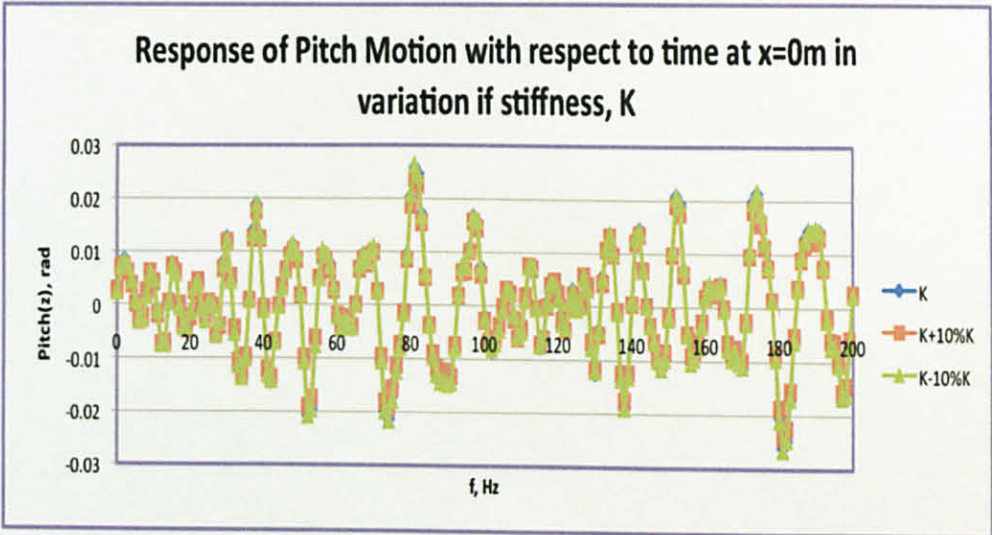


Figure 17: Simulated Pitch Profile (1)



## Variation of Hydrodynamic coefficient

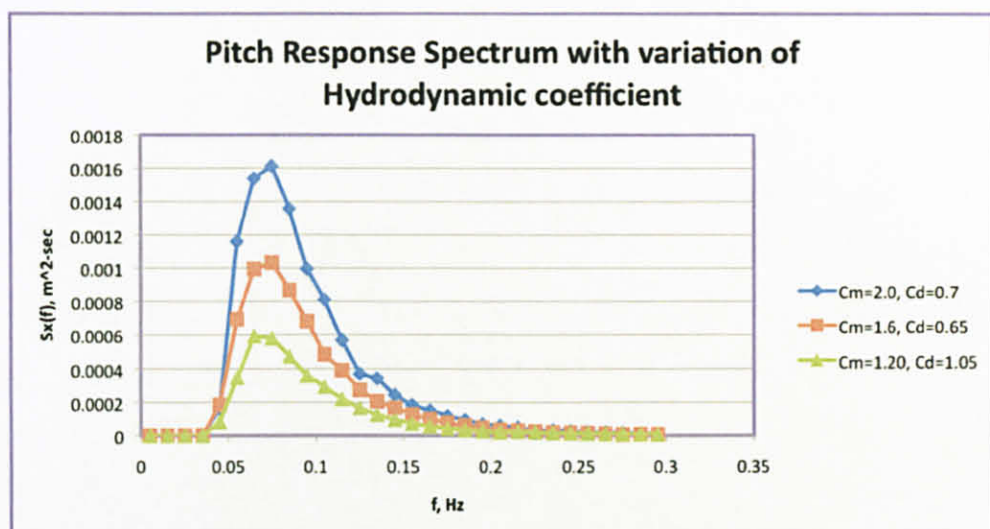


Figure 18: Pitch Response Spectrum (2)

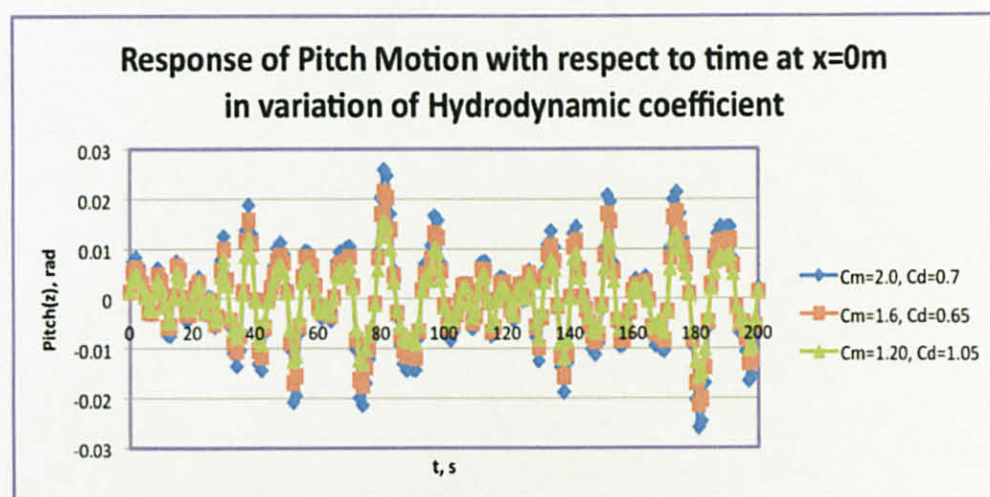


Figure 19: Simulated Pitch Profile (2)

From Figure 17, when the stiffness value varied from  $\pm 10\%$ , the maximum response is 0.0264 radian. The response increased by 8.1% when the stiffness value is decreased and the response was minimized approximately 1.9% at stiffness greater than the original. As for the variation in hydrodynamic coefficient, the highest response is 0.0259 radian when the  $C_m=2.0$ ,  $C_d=0.7$ . The percentage difference in

Clean condition is 17.4% and in Fouled condition, the response is largely decreased by 39.8%.

### **4.3. Discussions**

The wave profile of the truss spar was computed in an extreme condition at Gulf of Mexico. The analysis is subjected to a random waves in the range  $(0, 2\pi)$ . The predicted responses of truss spar were only measured approximately due to the following reasons:

- a. There is limitation of frequency domain technique that all nonlinearities in the equations of motions (Equation 12) were replaced by linear approximation.
- b. The mass moment inertia were calculated based on assumed distribution masses.

The value of  $K$  is varied to analyze the effect of stiffness to the total response of the spar. Change in stiffness will affect the total buoyancy of the structure; the draft changed and finally will affect the total motion response of spar. In this study, the spar stiffness was simplified by using static equilibrium conditions.

Hydrodynamic coefficients are essential in the computation of Morison's Equation and also in added mass. As stated in Equation 2, the value of  $C_m$  and  $C_d$  affect the total force that acting on the cylinder (spar). The inertia and drag force decreased as the value of the coefficient decreased.

## CHAPTER 5

### 5. CONCLUSION

The developed frequency domain analysis of a typical spar has been able to predict the responses in surge, heave and pitch degree of freedom when the spar was subjected to a random waves developed by P-M Spectrum. Responses in the two parametric stiffness and hydrodynamic coefficient were determined and the correspondence wave profiles are simulated.

From the numerical results, the percentage difference when the stiffness was increased to 10% is 9.66% for surge, 9% for heave and 1.9% for pitch, while the response is increase by 10.1% in surge, 11.3% in heave and 8.1% for pitch as the stiffness was decreased by 10% of its original stiffness. For hydrodynamic coefficient analysis, Clean condition, the response decreased by 20.7% in surge and 17.4% in pitch motion. The resulted responses in Fouled condition showed 40% reduction in surge response and 39.8% in pitch. The predictions using frequency domain are not very accurate as it cannot take the nonlinearities into account. However, the responses followed the same trend of the applied wave as shown by time domain results literature. The value of response increases as the stiffness decreased and the response decreases when the hydrodynamic coefficient decreases.

The lab experiment is used to see the typical truss spar response behavior in two conditions. The wave is generated by P-M spectrum.

The results of this frequency domain analysis can be very useful for the preliminary design of spar and its components.



CHAPTER 6

6. ECONOMIC BENEFITS

Spar design are the most economical for ultra deep water by utilizing a mooring system instead of permanent legs, spar platforms reduce materials cost and can be moved to different wells. Oryx spent \$300 million on Neptune, the world’s first production spar platform and have save Oryx and its 50/50 partner \$90 millions.

When compared to other floating structure, spar has great advantage on saving cost and time. Referring to the graph below, the construction of spar is less time consuming.

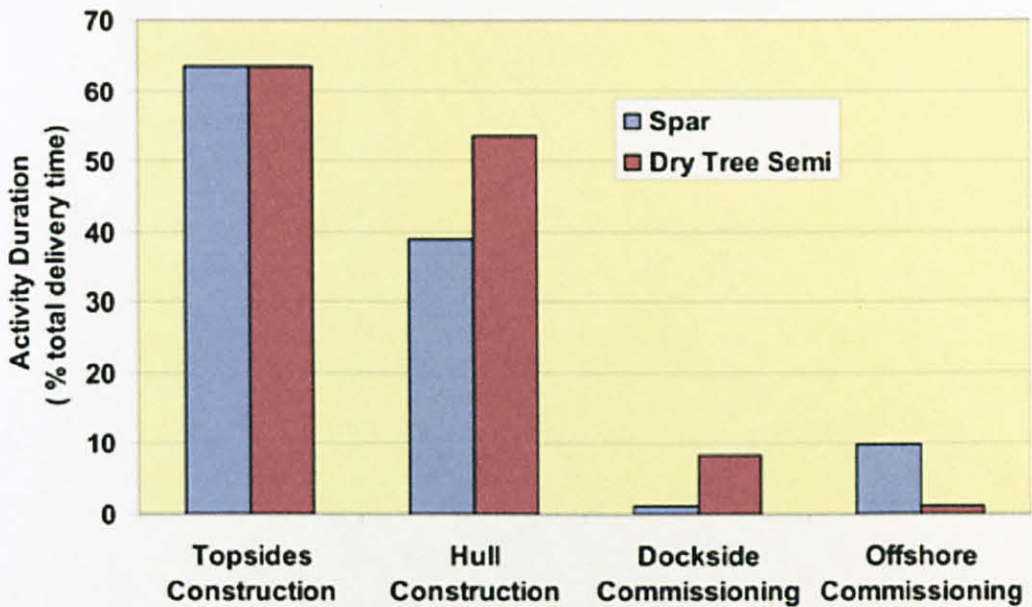


Figure 20: Comparison of construction time between spar and Dry tree semisub

The hull of truss spar is smaller, reducing both material and transportation cost. The Holstein spar is one example of truss spar and is the largest spar ever built. Truss spar has proven design, hull delivering on time and on cost (sometime less), consist of large payload capacity and be dry or wet solution.

According to Technip (2000), the delay in oil production is costly. For example;



6 months delay in first oil production;

180 days at \$6M/day = \$ 1080M

10% interest = \$90M

(Currency in US Dollar)

On time spar deliveries can save a lot of money. The construction of Holstein spar finished 4 months earlier than expected.

Finn Theorem explained that the costs of all platforms are the same and spar has advantage on risers completion, drilling and work over. Oil drilling from spar is effectively reducing the cost. Below are the cost comparisons.

*Table 4: Construction cost comparison*

	Jackup	Semisub	Spar
Transportation	100	100	100
Drilling	600	600	240
Complete	400	160	160
Surf	300	100	100
Topside	250	250	250
Platform	150	180	220
Total	1500	1400	1070

(US dollar)

Observation from the table can conclude that spar is more economical compared to the other platforms.

A lot of money is spent in designing and maintenance purposes, this study will help to further reduce the consultancy cost as it will help to determine the optimum design parameter. With effective spar design, it can reduce and save money and time.

## CHAPTER 7

### 7. REFERENCES

- [1] *Effects of Spar Coupled Analysis*, Himanshu Gupta, Spars International Inc.; Lyle Finn, Tim Weaver, Deep Oil Technology, Inc, Offshore Technology Conference, 1 May-4 May 2000, Houston, Texas
- [2] *Hydrodynamics of offshore structures*, S.K. Chakrabarti, 1997
- [3] *Comprehensive study on the linear hydrodynamic Analysis of a truss Spar in random waves*, Roozbeh Mansouri, Hassan Hadidi
- [4] *Numerical Models for SPAR Platform Dynamics*, Arne Nestegård, Marit Ronæss, Geir Skeie, Joar Dalheim and Torgeir Vada
- [5] *Vertical Motion Characteristics of Truss Spars in Waves*, Jun B. Rho and Hang S. Choi
- [6] *Handbook of offshore engineering*, Subrata K. Chakrabarti, Volume 1, 2005, Offshore structure analysis, Plainfield Illionis
- [7] *Diffraction method for spar platform*, C.Y. Ng, V.J Kurian, M. A. W Mohamed.
- [8] *Spar Global Responses 2001*, John Halkyard, CSO Aker Engineering, INC
- [9] *Heave and Pitch Motions of a Spar Platform with Damping Plate*, Jun B. Rho, Hang S. Choi, 2002, The International Society of Offshore and Polar Engineers
- [10] *Frequency Domain Analysis of Truss Spar Platform*, V.J. Kurian, BS Wong, O.A.A Montasir, ICCBT2008.
- [11] *Dynamic Response of Spar Platform subjected to waves and current*, V.J. Kurian, O.A.A Montasir, SP Narayanan, M.A.W. Mubarak, ICCBT 2008.

- [12] *Motions of a spar buoy in random seas: comparing predictions and model test*, Alok K. Jha, P.R. de Jong, Steven R, From proceedings, BOSS-97: Behavior of offshore structures volume 2 (Hydrodynamics), 1997
- [13] *Argarwal, A.K. & Jain, A.K. Dynamics behaviour of offshore spar platform under regular sea waves. Ocean Engineering 30, 2003. 487-516. 347.*
- [14] *Burke, B.G. & Tighe, J.T. A time series model for dynamics behaviour of offshore structures. 3<sup>rd</sup> Annual Offshore Technology Conference, Houston, Texas, 1972. OTC-1403*
- [15] *Graff, W.J. Introduction to offshore structures: design fabrication installation. Gulf Publishing Company. 1981. 69-71*
- [16] *Wang, J., Berg, S., Luo, H.Y., Sablok, A. & Finn, L. Structural design of the truss spar: an overview. Proceedings of the 11<sup>th</sup> International Offshore and Polar Engineering Stacanger, Norway, 2001. 354-361*
- [17] *Wang, J., Zhang, B. & Berg, S. Truss spar time domain inplace structural strength anylysis. Offshore Technology Conference, Houston, Texas, 2002. OTC-14299.*
- [18] *Vardeman RD, Richardson S, McCandless CR. Neptune Project: Overview and Project management. OTC 8381, Offshore Technology Conference, Houston, TX, USA. Vol. 2, 1997. P. 227-35.*
- [19] *Weggle DC, Rosset JM. Second order dynamics response of a large spar platform: numerical predictions versus experimental results. OMAE'96, Florence, Italy. Vol. 1, Part A, 1996. p. 489-96.*

# **APPENDIX I**

## **WAVE DATA**



Table 3.19 Typical sea states for various offshore locations around the world [adopted from DNV-OS-E01, 2001]

Description	Location	Type	$H_s$ m	$T_p$ s	$U$ m/s	$U_c$ m/s
Norwegian Sea	Hallenbanken		16.5	17.0	19.0	0.90
Northern North Sea	Troll field		15.0	15.5	17.5	1.50
North Sea	Greater Ekofisk field		14.0	15.0	17.0	0.55
Mediterranean	Libya	shallow water	8.5	14.0	1.00	25.3
	Egypt		12.1	14.4	0.78	25.1
Gulf of Mexico		Hurricane	11.9	14.2	1.98	44.1
West Africa	Nigeria	swell	3.6	15.9	1.1	16.0
	Nigeria	squalls	2.7	7.6		16.6
	Gabon	wind generated	2.0	7.0	0.91	24.1
	Gabon	swell	3.7	15.5		16.0
	Ivory Coast	swell	6.0	13.0	0.90 <sup>(1)</sup>	29.5
	Angola	swell, shallow water	4.1	16.0	1.85 <sup>(2)</sup>	21.8
South America	Brazil (Campos Basin)		8.0	13.0	1.60	35.0
Timor Sea	Non-typhoon		4.8	11.5	1.10	16.6
Timor Sea	Typhoon		5.5	10.1	1.90	23.2
South China Sea	Non-typhoon		7.3	11.1	0.85	28.6
	Typhoon		13.6	15.1	2.05	56.3

(1) Ocean current going to east

(2) Ocean current going to 347.5° approximately parallel to the coast

17

Table 3.20 Extreme design environment criteria for various locations

Location	Type	Water depth m	$H_s$ m	Wind speed m/s	Surface current m/s	Seabed current m/s	Current type
Gulf of Mexico	Hurricane	3000	12.9	42.0	1.1	0.1	bilinear
Gulf of Mexico	Loop	3000	4.9	32.9	2.57	0.51	bilinear
Brazil	Foz de Amazon	3000	6.0	20.0	2.5	0.3	bilinear
Northern Norway	Nyk High	1500	15.7	38.5	1.75	0.49	linear
West Africa	Girrasol	1350	4.0	19.0	1.5	0.5	bilinear
Atlantic Frontier	Faeroe-Shetland Channel	1000	18	40.0	1.96	0.63	linear

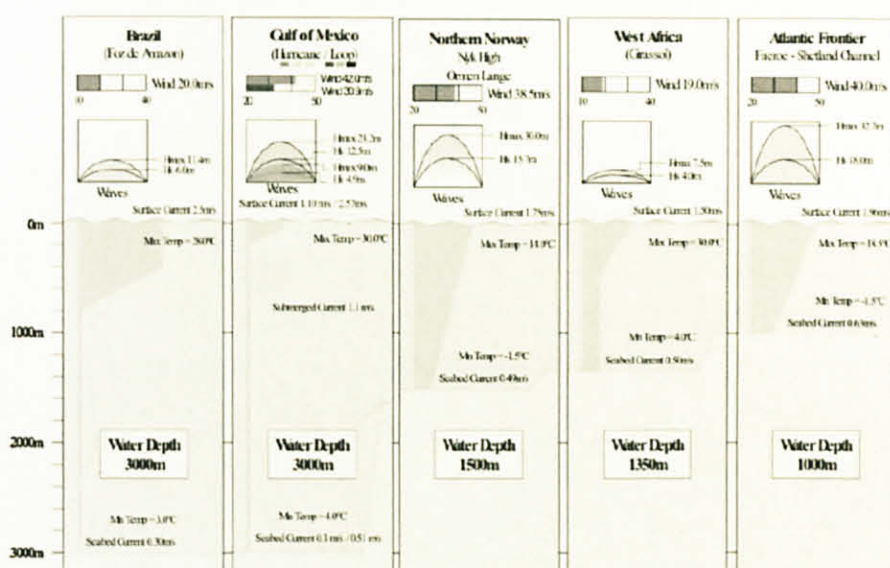


Figure 3.27 Environmental conditions at several deep water sites [Moros and Fairhurst, Offshore, April (1999), Courtesy BPI]

Table 3.21 Typical 100-yr environment [Halkyard, et al 2000]

Region	West Africa		Brazil		Gulf of Mexico	
Dominant environment	100 yr current*	100 yr storm*	100 yr current*	100 yr storm*	Loop current	Hurricane
Sig wave ht, ft	10.5	12.1	20.7	24.9	15.0	44.3
Peak period, s	15.0	15.1	12.1	12.7	9.0	14.6
JONSWAP $\gamma$	3.0	3.0	3.0	3.0	2.4	2.4
Wind 1h @ 10 m kts	33.8	41.8	49.6	57.0	30.0	84.2
Surface Current kts	2.00	1.79	3.79	3.15	4.00	2.10

\*Note: Current = 10 yr wind/wave and 100 yr current  
Storm = 100 yr wind/wave & 10 yr current

# **APPENDIX II**

## **WAVE SPECTRUM**

## Wave Spectrum

f	t	$\alpha \cdot g^2 \cdot f^{-5/2} \pi^4$	$\exp(-1.25 \cdot (f/f_0)^4)$	S(f)	H(f)	R	$\xi$
0.005	200	160049211.4	0	0	0	0.115	0.72256631
0.015	66.66666667	658638.7299	2.3788E-112	1.5667E-106	3.54034E-54	0.652	4.09663682
0.025	40	51215.74764	3.41645E-15	1.74976E-10	3.7414E-06	0.018	0.113097336
0.035	28.57142857	9522.770951	0.000171503	1.633180843	0.361461571	0.42	2.638937829
0.045	22.22222222	2710.447448	0.041872633	113.493572	3.013218505	0.671	4.216017341
0.055	18.18181818	993.7796808	0.241241671	239.7410704	4.379416129	0.447	2.808583832
0.065	15.38461538	431.0590595	0.482426783	207.9544354	4.078768789	0.296	1.859822851
0.075	13.33333333	210.7643936	0.66283001	139.7009652	3.343064046	0.161	1.011592834
0.085	11.76470588	112.7220638	0.779373443	87.85258298	2.651076505	0.981	6.163804786
0.095	10.52631579	64.6376463	0.852356335	55.09430729	2.099415296	0.567	3.562566069
0.105	9.523809524	39.18835782	0.898482283	35.2100452	1.678333583	0.06	0.376991118



**APPENDIX III**

**WAVE CALCULATION**

**TOTAL HORIZONTAL FORCE**

Wave Calculation – Total Horizontal Force for Hard Tank

hard dia tank, D	46	row	1030
wave height, Hmax	24	g	9.80665
water depth, d	1325	Cd	0.7
wave period, Tass	16.7	Cm	2
dist from origin, X	0	Cosh kd	100528513.9
time at x, t	0	H/2	12
omega, $\omega$	0.376238641	$\rho H/T$	4.514863694
wave length, L	435.44	$2\rho^2 H/T^2$	1.698666181
k	0.014429509	$(D/2)Cdr$	16583
$\theta$	0	$(\rho D^2/4)Cmr$	3423519.178
sinh kd	100528513.9		
sin theta	0		
cos theta	1		

y (m)	s	cosh ks	sinh ks	U	U <sub>o</sub>	Curnt. V	Drg Force	In.Force	T.FORCE (Fx), N
-1	1324.5	99805835.43	99805835.43	4.482407284	0	1.09961883	333185.2225	0	333185.2225
-2	1323.5	98376026.77	98376026.77	4.418192755	0	1.098856489	323707.2446	0	323707.2446
-3	1322.5	96966701.42	96966701.42	4.354898157	0	1.098094149	314498.8828	0	314498.8828
-4	1321.5	95577565.92	95577565.92	4.292510312	0	1.097331809	305552.4673	0	305552.4673
-5	1320.5	94208331.05	94208331.05	4.231016228	0	1.096569468	296860.5467	0	296860.5467
-6	1319.5	92858711.69	92858711.69	4.170403103	0	1.095807128	288415.8814	0	288415.8814
-7	1318.5	91528426.86	91528426.86	4.110658315	0	1.095044787	280211.4379	0	280211.4379
-8	1317.5	90217199.55	90217199.55	4.051769425	0	1.094282447	272240.3827	0	272240.3827
-9	1316.5	88924756.76	88924756.76	3.993724172	0	1.093520107	264496.0767	0	264496.0767
-10	1315.5	87650829.38	87650829.38	3.93651047	0	1.092757766	256972.0697	0	256972.0697
-11	1314.5	86395152.15	86395152.15	3.880116405	0	1.091995426	249662.0949	0	249662.0949
-12	1313.5	85157463.64	85157463.64	3.824530236	0	1.091233086	242560.0638	0	242560.0638

# **APPENDIX IV**

## **HEAVE ANALYSIS**



<b>H</b>	0.133711467
<b>D</b>	1325
<b>T</b>	3.389830508
<b>dia</b>	46
<b>t</b>	0
<b>omega</b>	1.853539666
<b>Lo</b>	17.9348098
<b>k</b>	0.35033465
<b>sinh kd</b>	1.9752E+201
<b>sin thea</b>	1
<b>cos theta</b>	0
<b>row</b>	1030
<b>g</b>	9.80665
<b>Cd</b>	0.7
<b>Cm</b>	2
<b>Cosh kd</b>	1.9752E+201
<b>H/2</b>	0.066855733
<b>pH/T</b>	0.123919754
<b>2p2H/T2</b>	0.229690179
<b>(D/2)Cdr</b>	16583
<b>(pD2/4)Cmr</b>	3423519.178

x	$\theta$	sin theta	cos theta	s	cosh ks	sinh ks	Pressure	Area	Fy, KN
0	0	0	1	1248	3.8035E+189	3.8035E+189	1.30038E-09	0	0
2.3	0.805769694	0.721363913	0.692556211	1248	3.8035E+189	3.8035E+189	9.00584E-10	10.58	9.52818E-12
4.6	1.611539388	0.999170116	-0.04073179	1248	3.8035E+189	3.8035E+189	-5.29667E-11	21.16	-1.12078E-12
6.9	2.417309083	0.662599026	-0.748974319	1248	3.8035E+189	3.8035E+189	-9.73949E-10	31.74	-3.09131E-11
9.2	3.223078777	0.081395975	-0.996681843	1248	3.8035E+189	3.8035E+189	-1.29606E-09	42.32	-5.48494E-11
11.5	4.028848471	0.775341602	-0.631542081	1248	3.8035E+189	3.8035E+189	-8.21243E-10	52.9	-4.34438E-11
13.8	4.834618165	0.992539309	0.121925062	1248	3.8035E+189	3.8035E+189	1.58549E-10	63.48	1.00647E-11

# **APPENDIX V**

## **PITCH ANALYSIS**

- i)    MOMENT  
CALCULATION**
- ii)   RAO MOMENT  
CALCULATION**

## i) Moment Calculation

S	Force, $f_x$ (N)	At depth, $y$ (m)	Moment arm (m)	Moment, $M$ (Nm)
1324.5	525745.4952	-0.5	65	34173457.19
1323.5	370362.3309	-1.5	64	23703189.18
1322.5	260902.4514	-2.5	63	16436854.44
1321.5	183793.2607	-3.5	62	11395182.16
1320.5	129473.5502	-4.5	61	7897886.56
1319.5	91207.92301	-5.5	60	5472475.381
1318.5	64251.62276	-6.5	59	3790845.743
1317.5	45262.19938	-7.5	58	2625207.564
1316.5	31885.05852	-8.5	57	1817448.336
1315.5	22461.5019	-9.5	56	1257844.106
1314.5	15823.05626	-10.5	55	870268.0944



ii) RAO Moment Calculation

Fx	1778.883473
H/2	0.066855733
Mt	2.36E+08
w	0.376238641
w^2	0.141555515
t	150
wn	0.041887902
wn^2	0.001754596
K	4.14E+05
C	9.89E+05
(K-Mw^2)^2	1.09E+15
(cw)^2	1.38E+11
upper	26607.79239
lower	32995113.17
RAO	0.000806416